



Use of peanut shell-based polyurethane type rigid foam in removing remazol orange RGB dye from aqueous solution

Bilal ACEMIOĞLU *

on the last page

Department of Chemistry, Faculty of Science and Arts, Kilis 7 Aralık University, 79000, Turkey

Received: 23 April 2020; Revised: 07 June 2020; Accepted: 09 June 2020

*Corresponding author e-mail: acemioğlu@kilis.edu.tr

Citation: Acemioğlu, B. *Int. J. Chem. Technol.* 2020, 4 (1), 79-89.

ABSTRACT

This study reflects the adsorption ability and usability of peanut shell-polyurethane type rigid foam for the removal of remazol orange RGB (RO-RGB) dye, a reactive dye, from aqueous solution. RO-RGB removal was studied for initial dye concentrations (10-150 mg l⁻¹), pH values (3-9), and temperatures (20-60°C) at various contact times. Dye removal increased with the increases in initial dye concentration and temperature while it was decreasing with an increase in pH. Maximum dye removal was determined to be about 98% under all the experimental conditions. Equilibrium data obtained were adapted to the Langmuir, Freundlich, and Temkin isotherm models, and it was seen that the adsorption obeyed the Freundlich isotherm model with determination of coefficient of $r^2 = 0.966$. Kinetics data was found to be harmony with the pseudo-second kinetic order model (higher than $r^2 = 0.9908$). As a result, it was determined that the polyurethane-type rigid foam produced from peanut shell could be used as an alternative to activated carbon and could easily be used as an adsorptive material to remove RO-RGB dye.

Keywords: Peanut shell, polyurethane type rigid foam, remazol orange RGB, removal, adsorption.

Remazol turuncu RGB boyasının sulu çözeltiden uzaklaştırılmasında fıstık kabuğu bazlı poliüretan tipi sert köpüğün kullanımı

ÖZ

Bu çalışma reaktif bir boyar madde olan remazol turuncu RGB (RO-RGB)'nin sulu çözeltiden uzaklaştırılması için yerfıstığı kabuğu esaslı poliüretan tipi sert köpüğün adsorpsiyon kabiliyetini ve kullanılabilirliğini yansıtmaktadır. RO-RGB uzaklaştırılması, çeşitli temas sürelerinde farklı konsantrasolar (10-150 mg l⁻¹), pH değerleri (3-9), ve sıcaklıklar (20-60°C) için incelenmiştir. Boya uzaklaştırılması pH daki bir artışla azalırken başlangıç boyar madde konsantrasyonu ve sıcaklıktaki artışlarla artmıştır. Maksimum boya uzaklaştırılmasının tüm deneysel şartlar altında yaklaşık % 98 civarında olduğu belirlenmiştir. Elde edilen denge dataları Langmuir, Freundlich, and Temkin isotherm modellerine uyarlanmıştır ve adsorpsiyonun $r^2 = 0.966$ 'lık bir belirlenme katsayısı ile Freundlich isotherm modeline uyduğu görülmüştür. Kinetik dataların yalancı ikinci dereceden kinetik model ile uyumlu olduğu bulunmuştur ($r^2 = 0.9908$ 'den daha büyük). Sonuç olarak, yer fıstığı kabuğundan üretilen poliüretan tipi sert köpüğün aktif karbona alternatif olarak kullanılabilmesi ve RO-RGB boyasının uzaklaştırılması için adsorptif bir malzeme olarak kolayca kullanılabilmesi belirlenmiştir.

Anahtar Kelimeler: Yerfıstığı kabuğu, poliüretan tipi sert köpük, remazol turuncu RGB, uzaklaştırma, adsorpsiyon.

1. INTRODUCTION

In today's world, where industrialization is increasing, environmental problems affect negatively human health. Especially the wastes of factories such as dyeing, ink, textile, automotive, paper, leather industries etc. cause

to many diseases such as allergy, dermatitis, cancer, mutation and skin irritation.¹ Therefore, it is extremely important to remove such undesired substances from the environment.² For this purpose the adsorption method, which is a cheap and effective method, has been commonly used recently. The adsorption method can

be described generally as the removal of dyes or metal ions from an aqueous medium using an adsorbent material. Activated carbon is used generally in adsorption method. However, since activated carbon is expensive, many scientists have used cheaper adsorbents recently.³ According to the literature search, some inexpensive adsorbents such as organic, inorganic, biological, and lignocellulosic materials which are used to effectively remove environmental pollutants are listed below. For example, poly(N-isopropylmethacrylamide-acrylic acid) microgels⁴ and polydopamine microspheres⁵ as organic adsorbents; zinc oxide,⁶ perlite,⁷ clay⁸ as inorganic adsorbents; fungus,^{9,10} algae¹¹ and yeast¹² as biological materials; coconut sawdust,³ shells,¹³ watermelon rind,¹⁴ tree barks,^{15,16} wheat straw,¹⁷ orange peel,¹⁸ and peanut shell,¹⁹ as lignocellulosic materials have been used.

Of these, the adsorbents with lignocellulosic content are natural agricultural wastes with no economic value. Such materials have been used directly in the literature for dye and metal adsorption, but they usually do not show very high adsorption capacity. In order to increase the adsorption capacity, lignocellulosic adsorbents have been used either by modifying or by producing new adsorbent materials. According to the literature survey, new adsorbents produced from lignocellulosic materials can be listed as: phenolated wood resin,²⁰ Polyurethane cross-linked pine cone biomass,²¹ lignin-based hydrogels,²² the polyurethane type rigid foam produced from peanut shell. Our previously some studies can be expressed as follows, respectively.

Removal of remazol orange RGB (RO-RGB) using biochar produced from peanut shell has been studied.²³ Adsorption of safranin-O dye²⁴ using peanut shell-based polyurethane type foam (PSPUF) pretreated with HCl has been investigated. Also, PSPUF obtained by chemical modification with HCl has been used for the adsorption of remazol brilliant blue R.²⁵ However, no study has been reported for RO-RGB removal by this foam in the literature. Therefore, in this study, the use of PSPUF for RO-RGB removal from aqueous solution is aimed. Thus, the present paper reflects an original study. Effects of contact time, initial dye concentration, temperature, and pH on dye removal are investigated. Moreover, isotherm, kinetics and thermodynamic studies for dye removal are also performed.

2. EXPERIMENTAL

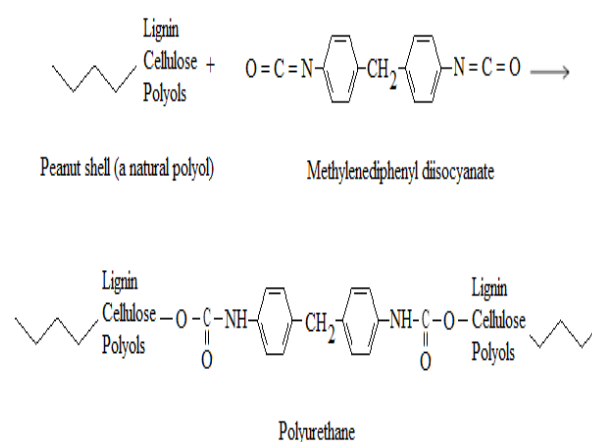
2.1. The supply of raw material peanut shell for the production of polyurethane type rigid foam

In order to obtain the polyurethane-type rigid foam from peanut shell, the peanut shell wastes were received from

Osmaniye province of Turkey. Firstly the samples were cleaned well and then dried in an oven until a constant weight. Dried samples were powdered by a grinding mill, and stored after sieving over 100-mesh molecular sieve to produce polyurethane-type rigid foam.

2.2. Preparation of peanut shell-based polyurethane type rigid foam for dye removal

PSPUF was produced from a reaction between the peanut shell and methylene diphenyl diisocyanate (MDI) via polyaddition polymerization as described in our previous study. The formation of PSPUF using the foam and MDI is shown in Scheme 1.²⁴



Scheme 1. The formation of polyurethane-type rigid foam using peanut shell and methylenediphenyl diisocyanate (MDI).

PSPUF was modified for dye removal experiments because the resulting foam did not adsorb RO-RGB dye. Modification was carried out by chemically reacting the foam with HCl at 140°C for 6 h. This reaction was performed using 10 g foam and 10 ml 0.5 N HCl. After the reaction time of 6 h, the reaction mixture was filtered and then the modified PSPUF was washed well with distilled water to clear impurities.²⁵

2.3. Characterization of the foam

Specific BET surface area and porosity, elemental analysis, density measurement, FT-IR and SEM analyses were performed for characterization of the foam. Specific BET surface area and porosity was determined using Micromeritics ASAP® 2420 device. Elemental analysis was carried out by a LECO CHNS-932 analyzer. Density measurement was performed using a graduated tape measure. FT-IR measurements were recorded between 4000 and 650 cm^{-1} wavenumbers by a ATR spectrophotometer. SEM analysis was recorded by a LEO 435 VP SEM brand device.

2.4. Supply of the dye

RO-RGB was provided from Dystar. Since this dye is a new generation of reactive dyes for medium to deep shades, its structure has been protected by manufacturer firm. This dye was analyzed using a spectrophotometer by us and its absorption spectra for various concentrations are illustrated in Figure 1.²³ The maximum wavelength of this dye was determined to be 478 nm.

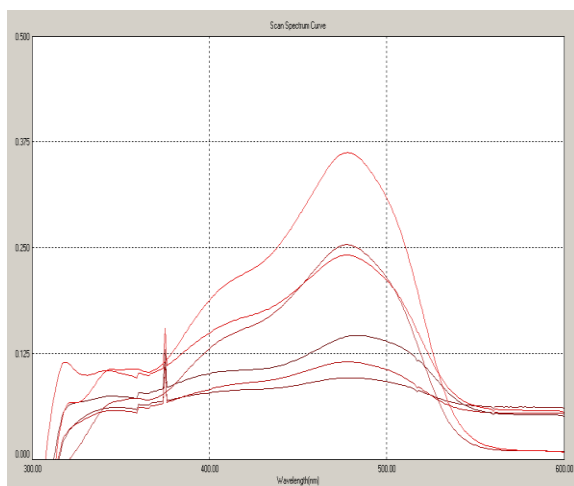


Figure 1. UV-Vis spectra of RO-RGB for different initial concentrations (top to bottom concentrations: 150, 100, 75, 50, 20 and 10 mg l⁻¹).

2.5. Preparation of dye solutions

The RO-RGB was used as taken. Firstly the stock solution of 500 mg l⁻¹ of RO-RGB dye was obtained using pure water. Then the working concentrations were prepared diluting the stock solution. pH values of solutions were regulated using diluted NaOH and HCl solutions by a pH meter (Elmetron pH Meter)

2.6. Removal experiments

Batch experiments were performed with 0.10 g foam and 50 ml dye solution using a temperature-controlled shaking water bath under all the experimental conditions. After shaking at 130 rpm for various times, the samples were centrifuged at 5000 rpm for 5 min by taking from shaking bath. The concentration of dye unadsorbed in the supernatant was determined by a T80 UV/Vis spectrometer at $\lambda_{\max} = 478$ nm. The percent removal and the dye amount removed (q_t) were estimated using Equations (1) and (2), respectively:

$$\text{Removal \%} = (C_0 - C_e / C_0) \cdot 100 \quad (1)$$

$$q_t = (C_0 - C_t) V / m \quad (2)$$

Where, C_0 (mg l⁻¹) indicates the initial dye concentration. C_e and C_t (mg l⁻¹) refer the dye concentrations at equilibrium and any time, respectively. q_t (mg g⁻¹) shows the amount of RO-RGB removed by unit mass of adsorbent at any time. V (l) refers to the volume of the RO-RGB solution. m (g) shows the mass of the foam. At the equilibrium time, q_t is equal to q_e , and C_t is equal to C_e (mg l⁻¹).

3. RESULTS AND DISCUSSION

3.1. Characterization of PSPUF

Some physical properties of the foam have been given in our previous study.²⁵ As seen in this study, the values we obtain are as follows: Specific BET surface area and porosity of the peanut shell-based-polyurethane type rigid foam are 2.824 m² g⁻¹ and 0.00215 cm³ g⁻¹, respectively. The color of the foam is brownish, and its density is 0.0341 g cm⁻³. According to elemental analysis results, the percent components of the modified foam are 61.20% C, 5.848% H, 6.975% N, and 0.274% S.

Figure 2 shows SEM image of the modified PSPUF. From this figure, it is seen that the surface of the foam has a porous, rough and heterogeneous structure which will adsorb dye molecules. It is determined from the isotherm studies that the adsorption on heterogeneous surface best fits the Freundlich model. This indicates a random adsorption (i.e. local adsorption) on the heterogeneous surface of the foam.

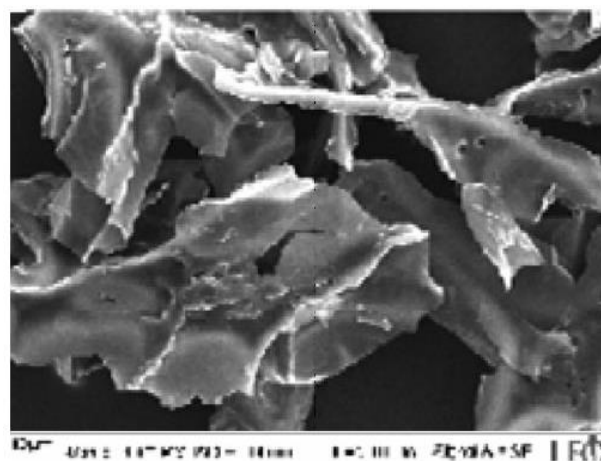


Figure 2. SEM image of the modified PSPUF.

FT-IR spectra for the determination of functional groups of the foam, modified foam and dye-adsorbed foam are shown in Figure 3.

Carefully looking at [Figure 3](#), it is seen that some peaks shift or disappear after modification and adsorption, and the intensities of some peaks are also decreased. All these changes are summarized in [Table 1](#).

It may be concluded from [Table 1](#) that the decrease or disappear or shift of intensity of some peaks points to a physical adsorption between the dye molecules and the foam.²

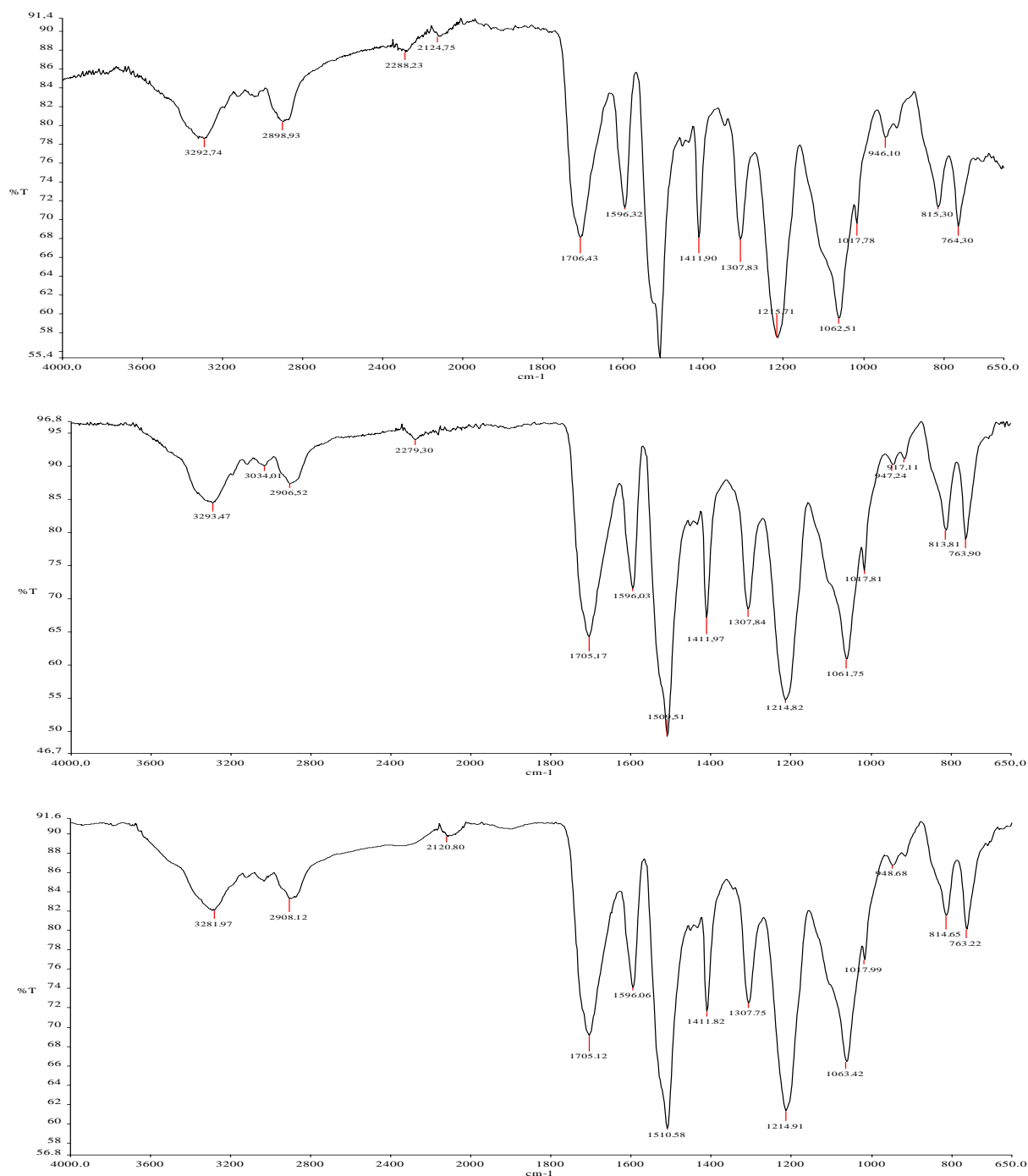


Figure 3. FT-IR spectra of: a) the foam, b) the foam modified with HCl, c) adsorbed dye on modified foam.

Table 1. FT-IR results

Functional groups	Before adsorption*	After modification with HCl	After adsorption
-OH in cellulose and NH and NH ₂ groups	3292.74 cm ⁻¹ (broad band)	3293.47 cm ⁻¹ (slightly shifted)	3281.97 cm ⁻¹ , Band shifted and intensity slightly decreased.
-CH stretching of carboxyl group	2898.93 cm ⁻¹	2906.52 cm ⁻¹ (very slightly shifted)	2908.12 cm ⁻¹ (very slightly shift)
C=C stretching groups	2124.75 cm ⁻¹	Diminished	2120.80 cm ⁻¹ (reappeared)
Amide I and amide II groups	1706.43 cm ⁻¹ , 1596.32 cm ⁻¹	Unchanged	Unchanged
Phenyl fragment	1411.90 cm ⁻¹	Unchanged	Unchanged
-CH ₂ (methylene group)	1307.83 cm ⁻¹	Intensity decreased.	1307.75 cm ⁻¹ (very slightly shifted)
-C-O and -C-O-C stretching groups	1062.51 and 1017.78 cm ⁻¹ (very strong peaks)	1061.75 cm ⁻¹ (Peak at 1062.51 very slightly decreased and shifted)	1063.41 cm ⁻¹ (very slightly shifted)
-C=O stretching of carboxylic group	1215.71 cm ⁻¹ (strong band)	1214.82 (very slightly shifted)	1214.91 (very slightly shifted)
-O-H bending	946.30 cm ⁻¹	947.20 cm ⁻¹ (very slightly shifted and intensity decreased)	948.68 cm ⁻¹ (very slightly shifted)
C-H out-of-plane bending	764.30 cm ⁻¹	763.90 cm ⁻¹ (very slightly shifted)	763.22 cm ⁻¹ (very slightly shifted)

3.2. Contact time effect and equilibrium time determination

Contact time effect on RO-RGB removal by the foam was studied for the conditions of various initial dye concentration, temperature and pH, respectively. In the case of initial dye concentration effect, the equilibrium time was attained at shorter times for lower concentrations and at longer time for higher concentrations. For instance, the equilibrium time was estimated to be 30 min for the initial dye concentrations of 10 and 20 mg l⁻¹, and 60 min for 50 mg l⁻¹. The equilibrium times were estimated to be 100, 150, and 300 minutes for 75, 100 and 150 mg l⁻¹, respectively. In the case of pH effect, the equilibrium time was determined as 60 min for all pH values for 50 mg l⁻¹. In the case of temperature effect, for 50 mg l⁻¹ at pH 3, the equilibrium times were determined to be 150 min for the temperatures of 20 and 30°C, 100 min for the temperatures of 40 and 50°C, and 60 min for the temperature of 60°C. A similar result has also been found for RO-RGB adsorption on peanut shell.²⁶

3.3. Initial dye concentration effect

Initial dye concentration effect on RO-RGB removal by the foam was studied for the concentrations of 10, 20, 50, 75, 100 and 150 mg l⁻¹ at pH 3, 60°C and 130 rpm. The results are graphed in Figure 4.

Herein, it is seen that the maximum dye removal (i.e. dye removal at equilibrium time) occurs at shorter time for lower initial dye concentration and at longer time for higher initial dye concentration. A similar trend has also been found for the removal of light green dye by cationic surfactant-modified peanut husk.²⁷ Herein, the maximum dye removals were determined as 0.98 mg g⁻¹ (98.60%) and 1.88 mg g⁻¹ (94.05%) for 10 and 20 mg l⁻¹ at the equilibrium time of 30 min. On the other hand, the maximum dye removals were estimated to be 4.56 mg g⁻¹ (91.24%), 5.56 mg g⁻¹ (74.20%), 7.294 mg g⁻¹ (72.94%) and 10.62 mg g⁻¹ (70.77%) for 50, 75, 100 and 150 mg l⁻¹ at the related equilibrium times, respectively.

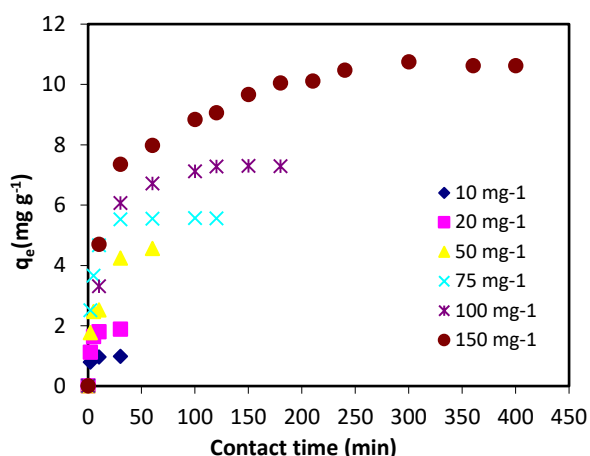


Figure 4. Initial dye concentration effect on RO-RGB removal by the foam.

From these results, it is seen that the dye removal is highly dependent on contact time and initial dye concentration. These values show that the percent dye removal is higher at lower initial concentration. This situation indicates that the dye will initially be adsorbed by more sites on the adsorbent surface. A similar result has also found for methylene blue removal using activated carbon obtained from *Cucumis sativa fruit peel*.²⁸

3.4. pH effect

pH effect on RO-RGB removal by the foam was studied at pH values of 3, 5, 7 and 9 for 50 mg l⁻¹ at 60°C and 130 rpm. The results are graphed in Figure 5.

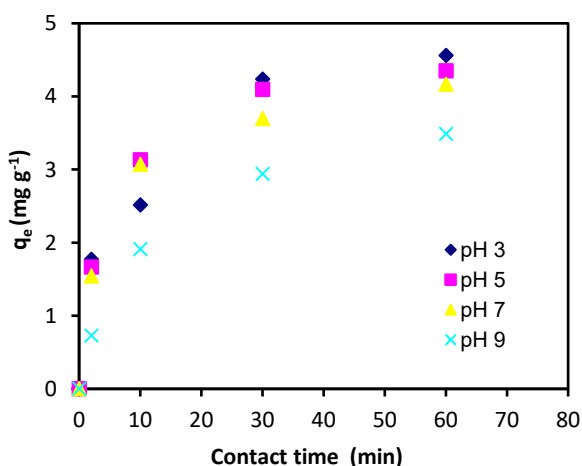


Figure 5. pH effect on RO-RGB removal by the foam.

Herein, it is seen that the dye removal increases with decreasing pH values (namely, with acidic pH). For example, the maximum dye removals were determined as 4.52 mg g⁻¹ (91.24%), 4.35 mg g⁻¹ (86.98%), 4.17 mg

g⁻¹ (83.36%) and 3.48 mg g⁻¹ (69.76%) for pH values of 3, 5, 7 and 9, respectively.

The dye removal of 91% to 69% between pH 3 and pH 9 indicates that pH has an important effect on dye removal. The fact that the dye removal is higher at lower pH value refers that a more electrostatic interaction occurs between more positively charged foam and negatively charged RO-RGB in acidic medium. A similar result has also been obtained for the removal of remazol brilliant blue R from aqueous solution using peanut shell pretreated with HCl.¹⁹

3.5. Temperature effect

Temperature effect on RO-RGB removal by the foam was worked at the temperatures of 20, 30, 40, 50 and 60°C for 50 mg l⁻¹ at pH 3 and 130 rpm. The results are graphed in Figure 6. Herein, dye removal increases with an increase in temperature, indicating an endothermic process. For instance, the maximum dye removals were determined as 1.30 mg g⁻¹ (26%), 2.78 mg g⁻¹ (55.66%), 2.82 mg g⁻¹ (56.56%), 3.17 mg g⁻¹ (63.34%), and 4.56 mg g⁻¹ (91.24%) for 20, 30, 40, 50, and 60°C. The fact that the dye removal is greater at higher temperature indicates both the enlarged of the foam particles and the increase in the mobility of the large dye ion with an increase in temperature. A similar result has been obtained for remazol brilliant blue R adsorption onto peanut shell-based polyurethane type foam.²⁵

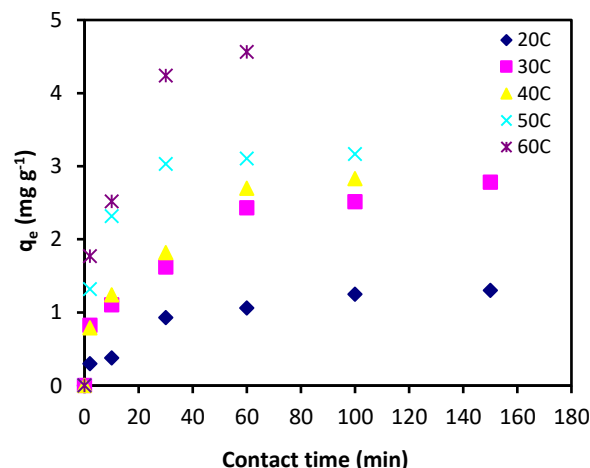


Figure 6. Temperature effect on RO-RGB removal by the foam.

3.6. Isotherm study

The adsorption equilibrium data were adapted to the Langmuir, Freundlich and Temkin isotherm models.

The linearized equations for these isotherms are expressed as follows.²⁹

$$C_e/q_e = 1/Q_0 \cdot b + C_e/Q_0 \quad \text{Langmuir} \quad (3)$$

$$\ln q_e = \ln k + 1/n \ln C_e \quad \text{Freundlich} \quad (4)$$

$$q_e = B \ln A + B \ln C_e \quad \text{Temkin} \quad (5)$$

Where, q_e (mg g⁻¹) shows the amount of dye removed by unit gram of the foam at the equilibrium time. C_e (mg l⁻¹) indicates the equilibrium concentration of dye remained in solution. Q_0 (mg g⁻¹) and b (l mg⁻¹) indicate Langmuir constants indicating adsorption capacity and energy, respectively. k (mg g⁻¹) and n (g l⁻¹) refer Freundlich isotherm constants indicating adsorption capacity and intensity, respectively. B (J mol⁻¹) is equal to RT/b_T , and it denotes the heat of the adsorption. b_T refers Temkin constant, A_T (l g⁻¹) indicates equilibrium binding constant.

The Q_0 and b values were estimated from the slope and intercept of the plot of C_e/q_e vs C_e , respectively. The k and n values were determined from the intercept and slope of the plot of $\ln q_e$ vs $\ln C_e$, respectively. The B and A_T values were calculated from the slope and intercept of the plot of q_e vs $\ln C_e$, respectively. All of the isotherm plots drawn are shown in Figure 7. The isotherm parameters were determined from the regression analyses of the plots in the figure. All parameters are presented in Table 2. The values of the determination of coefficient (r^2) were determined as 0.864, 0.966, and 0.824 for the Langmuir, Freundlich, and Temkin models, respectively. The isotherm results indicate that dye adsorption is the best consistent with Freundlich model with $r^2 = 0.966$. The compliance of the adsorption to the Freundlich model indicates the heterogeneous surface of the foam and a random adsorption on the surface. A similar result has also been found for remazol brilliant blue R adsorption onto peanut shell.¹⁹

Table 2. Isotherm parameters

Langmuir	Freundlich	Temkin
$Q_0 = 10.46$ (mg g ⁻¹)	$k = 2.05$ (mg g ⁻¹)	$B = 1.483$ (J mol ⁻¹)
b (l mg ⁻¹) = 0.147	n (g l ⁻¹) = 2.50	A_T (l g ⁻¹) = 6.481
$r^2 = 0.864$	$r^2 = 0.966$	$r^2 = 0.824$

3.7. Kinetic study

Kinetic studies of dye removal were performed according to three kinetic models used commonly. The

linear equations of these kinetic models are given in the following. The linear equation of the pseudo-first order kinetic model of Lagergren³⁰ is

$$\log (q_e - q_t) = \log q_e - \frac{k_1}{2.303} t \quad (6)$$

The linear equation of the pseudo-second order kinetic model of Ho³¹ is

$$\frac{t}{q_t} = \frac{1}{h} + \frac{1}{q_e} t \quad (7)$$

The linear equation of the intra-particle diffusion model of Weber and Morris³² is

$$q_t = k_i \cdot t^{1/2} \quad (8)$$

Where, k_1 , k_2 and k_i indicate the rate constants for the pseudo-first order (PFO), pseudo-second order (PSO) and the intra-particle diffusion models, respectively. q_e and q_t show the amounts of dye adsorbed per unit gram of the foam at the equilibrium and any time, respectively. h is the initial adsorption rate, it is equal to $k_2 q_e^2$. Herein, the plots of $\log (q_e - q_t)$ against t for the PFO model; the plots of t/q_t against t for the PSO model; the plots of q_t vs $t^{1/2}$ for intra-particle diffusion model are drawn. The all plots obtained are illustrated in Figure 8.

All of isotherm parameters obtained from regression analyses of these plots are submitted in Table 3. From linear regression analyses of the PFO plots, the r^2 values were determined as 0.8625, 0.9768, 0.9723, 0.881, 0.9618 and 0.9544 for 10, 20, 50, 75, 100 and 150 mg l⁻¹, respectively. For the PSO plots, the r^2 values were found as 0.9999, 0.9995, 0.9908, 0.9997, 0.999 and 0.9996 for 10, 20, 50, 75, 100 and 150 mg l⁻¹, respectively. For the intra-particle diffusion plots, the r^2 values were estimated to be 0.5789, 0.6604, 0.9377, 0.7086, 0.791 and 0.9177 for 10, 20, 50, 75, 100 and 150 mg l⁻¹, respectively.

The values from the PSO model were the most, and they were found to be higher than 0.999. On the other hand, because the values of q_t from the PFO kinetics model do not obey the experimental data, $q_e(\text{exp})$, even though the r^2 for some initial concentrations have high values (see Table 3), the adsorption does not obey this model.

The q_2 values from the PSO kinetic model are harmony with the $q_e(\text{exp})$, and thus the adsorption follows the PSO kinetics. A similar result has also been found for reactive blue 19 adsorption onto grafted chitosan.³³ This situation may be attributed to a chemical activation between RO-RGB molecules and the functional groups of the foam.

Moreover, because of the low values of the r_i^2 , it may be also said that the adsorption process does not follow the intra-particle diffusion kinetics.

3.8. Thermodynamic study

Thermodynamic parameters for RO-RGB adsorption were determined in the range of 20 and 60°C. The change in standard free energy (ΔG°), enthalpy (ΔH°),

and entropy (ΔS°) of adsorption were estimated from Equations (9-11).²⁹

$$K_c = C_{Ae} / C_{Se} \tag{9}$$

$$\Delta G^\circ = RT \ln K_c \tag{10}$$

$$\ln K_c = -\Delta H^\circ / RT + \Delta S^\circ / R \tag{11}$$

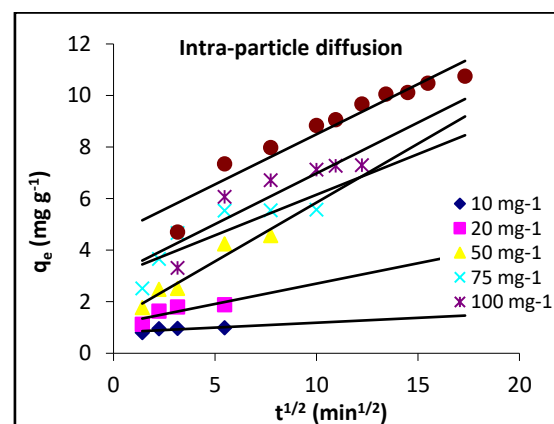
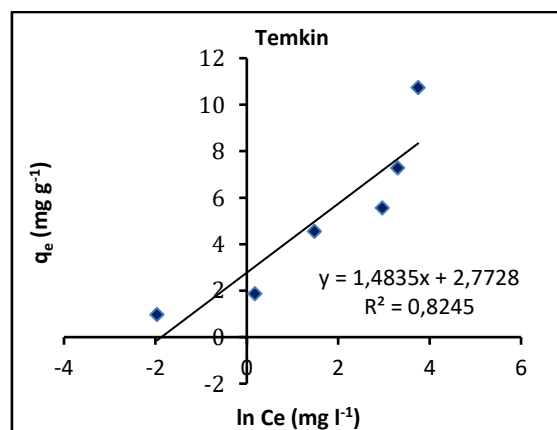
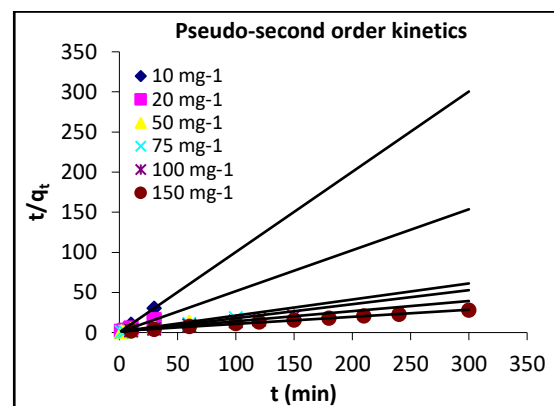
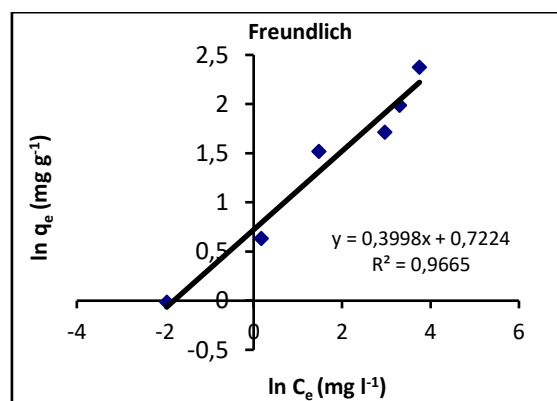
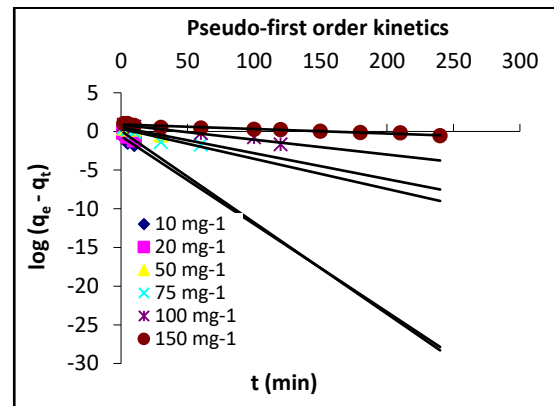
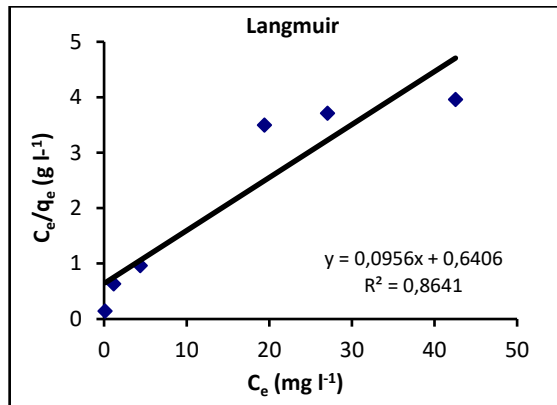


Figure 7. Isotherm plots.

Figure 8. Kinetic plots at different concentrations.

Table 3. Kinetic parameters

PSO					PFO		Intra-particle Diffusion			
C_0^a	q_2^b	k_2^c	h^d	r_2^{2e}	q_1^f	k_1^g	r_1^{2h}	k_i^i	r_i^{2j}	q_e^k
10	0.997	2.396	0.3941	0.9999	0.233	0.261	0.8625	0.0378	0.5789	0.98
20	1.159	0.440	0.5923	0.9995	0.414	0.272	0.9768	0.1579	0.6684	1.88
50	4.997	0.047	1.1881	0.9908	0.292	0.077	0.9723	0.4563	0.9377	4.56
75	5.717	0.012	0.3867	0.9997	0.128	0.089	0.881	0.3151	0.7086	5.56
100	7.911	0.022	1.4346	0.999	0.743	0.044	0.9618	0.3590	0.7910	7.29
150	11.363	0.015	1.9529	0.9996	0.810	0.133	0.9544	0.3888	0.9177	10.62

^aInitial dye concentration (mg l^{-1}).

^bEquilibrium adsorption capacity from the PSO equation (mg g^{-1}).

^cThe rate constant from the PSO model (g/mg min).

^dThe initial adsorption rate from the PSO kinetics (mg/g min).

^eDetermination of coefficient from the PSO kinetics (mg/g min).

^fEquilibrium adsorption capacity of the PFO model (mg g^{-1}).

^gThe rate constant from the PFO model (min^{-1}).

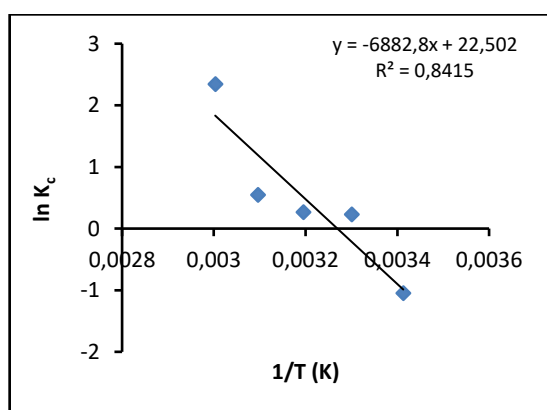
^hDetermination of coefficient from the PFO kinetics.

ⁱIntra-particle diffusion rate ($\text{mg/g min}^{1/2}$).

^jDetermination of coefficient from the intra-particle diffusion.

^kExperimental adsorption capacity at equilibrium time (mg g^{-1}).

Where, K_c shows adsorption equilibrium constant. C_{Ae} (mg l^{-1}) is the equilibrium concentration of dye adsorbed on the foam. C_{Se} (mg l^{-1}) is the concentration of RO-RGB remained in solution at the equilibrium time. R refers to the gas constant. T shows the absolute temperature. Eq. (11) refers Van't Hoff equation. Van't Hoff plot of $\ln K_c$ vs $1/T$ is shown in Figure 9.

**Figure 9.** Van't Hoff plot.

The ΔH° and ΔS° values were determined from the slope and intercept of Van't Hoff plot, respectively. All of the thermodynamic parameters are presented in Table

4. Herein, the ΔH° and ΔS° values were determined as $55.56 \text{ kJ mol}^{-1}$ and $187 \text{ J mol}^{-1}\text{K}^{-1}$, respectively.

The positive ΔH° value refers an endothermic adsorption. Since the ΔH° value is lower than 80 kJ mol^{-1} , the adsorption indicates a physical-chemical adsorption.³⁴ The positive ΔS° value indicates a random adsorption.

Table 4. Thermodynamic parameters

Temperature (in K)	K_c	ΔG° (J mol^{-1})	ΔH° (kJ mol^{-1})	ΔS° ($\text{kJ mol}^{-1}\text{K}^{-1}$)
20	0.351	2547		
30	1.255	-573	55.56	0.187
40	1.302	-687		
50	1.727	-1468		
60	10.415	-6488		

The negative ΔG° values for temperatures (except for 20°C) refer spontaneous adsorption of RO-RGB on the foam. The ΔG° values regularly decrease with an

increase in the temperature. This situation shows the increase of spontaneous trend with an increase in the temperature. Similar results have also been obtained for methylene blue adsorption on ZnCl₂ activated carbon prepared from wood apple outer shell.³⁵

4. CONCLUSIONS

The following conclusions were concluded from this study.

- Polyurethane type rigid foam prepared from the peanut shell was used as a low-cost adsorbent for RO-RGB removal from aqueous solution.
- RO-RGB removal was studied for various initial dye concentrations, temperatures, and pH values as function of contact time. The dye removal increased with the increases in initial dye concentrations and temperature, and with a decrease in pH. Under all the experimental conditions, the maximum dye removal was determined to be about 98%.
- Adsorption obeyed best the Freundlich isotherm model with the determination of coefficient of 0.966.
- The kinetics data was in harmony with the PSO model with the determination of coefficients higher than 0.9908.

As a result, it was concluded that the polyurethane-type hard foam produced from peanut shell will be used as a potential adsorbent as an alternative to activated carbon to remove other dye contamination besides RO-RGB removal from the environment.

ACKNOWLEDGEMENTS

This study was supported by The Scientific and Technical Research Council of Turkey (TUBITAK), project number: 107Y043.

Conflict of interests

Author declare that there is no a conflict of interest with any person, institute, company, etc.

REFERENCES

1. Acemioğlu, B. *J. Colloid Interf. Sci.* **2004**, 274, 371-379.
2. Aljeboree, A. M.; Alshirifi, A. N.; Alkaim, A. F. *Arab. J. Chem.* **2017**, 10, S3381-S3393.
3. El-Aila, H. J.; Elsouly, K. M.; Hartany, K. A. *Arab. J. Chem.* **2016**, 9, S198-S203.
4. Naseem, K.; Farooqi, Z. H.; Begum, R.; Ghufuran, M.; UrRehman, M. Z.; Najeeb, J.; Irfan, A.; Al-Sehemi, A.G. *J. Mol. Liq.* **2018**, 268, 229-238.
5. Fu, J.; Xin, Q.; Wu, X.; Chen, Z.; Yan, Y.; Liu, S.; Wang, M.; Xu, Q. *J. Colloid Interf. Sci.* **2016**, 461, 292-304.
6. Zhang, F.; Lan, J.; Yang, Y.; Wei, T.; Tan, R.; Song, W. *J. Nanopart. Res.* **2013**, 15, Article number: 2034.
7. Acemioğlu, B. *Chem. Eng. J.* **2005**, 106, 73-81.
8. Adeyemo, A. A.; Adeoye, I. O.; Bello, O. S. *Appl. Water Sci.* **2017**, 7, 543-568.
9. Acemioğlu, B.; Kertmen, M.; Digrak, M.; Alma, M.H.; Temiz, F. *Asian J. Chem.* **2010**, 22 (2), 1394-1402.
10. Bankole, P.O.; Adekunle, A.A.; Govindwar, S.P. *J. Environ. Chem. Eng.* **2018**, 6(2), 1589-1600.
11. Errgene, A.; Ada, K.; Tan, S.; Katircioğlu, H. *Desalination* **2009**, 249, 1308-1314.
12. Martorell, M. M.; Pajot, H. F.; de Figueroa, L. I. C. *J. Environ. Chem. Eng.* **2017**, 5987-5993.
13. Józwiak, T. C.; Filipkowska, U.; Bugajska, P.; Kalkowski, T. *J. Ecol. Eng.* **2018**, 19 (4), 129-135.
14. Husein, D. Z.; Aazam, E.; Battia, M. *Arab. J. Sci. Eng.* **2017**, 42, 2403-2415.
15. Acemioğlu, B.; Alma, M. H.; Demirkıran, A. R. *J. Chem. Soc. Pak.* **2004**, 26 (1), 82-89.
16. Rajamohan, N.; Rajasimman, M.; Rajeshkannan, R. R.; Saravanan, V. *Alexandria Eng. J.* **2014**, 53, 409-415.
17. Guo, Y.; Zhu, W.; Li, G.; Wang, X.; Zhu, L. *J Chem-NY*, **2016**, Article ID 6326372.
18. Kule, L.; Acemioğlu, B.; Baran, E. *Int. J. Chem. Technol.* **2017**, 1, 58-66.
19. Acemioğlu, B.; Sakalar, N. *Fresen. Environ. Bull.* **2017**, 26 (8), 5305-5313.
20. Kara, A.; Acemioğlu, B.; Alma, M.H.; Cebe, M. *J. Appl. Polym.* **2006**, 101, 2838-2846.
21. Kupeta, A. J. K.; Naidoo, E. B.; Ofomaja, A. E. *J. Clean. Prod.* **2018**, 179, 191-209.

22. Domínguez-Robles, J.; Peresin, M.S.; Tamminen, T.; Rodríguez, A.; Jääskeläinen, A.S. *Int. J. Biol. Macromol.* **2018**, 115, 1249-1259.
23. Acemioğlu, B. *Int. J. Coal Prep. Util.* DOI: 10.1080/19392699.2019.1644326
24. Acemioğlu, B.; Bilir, M. H.; Alma, M. H. *Int. J. Chem. Technol.* **2018**, 2 (2), 95-104.
25. Bilir, M. H.; Sakalar, N.; Acemioğlu, B.; Baran, E.; Alma, M. H. *J. Appl. Polym. Sci.* **2013**, 6, 4340-4350.
26. Samil, A.; Acemioğlu, B.; Gültekin, G.; Alma, M. H. *Asian J. Chem.* **2011**, 23 (7) 3224-3230.
27. Zhao, B.; Xiao, W.; Shang, Y.; Zhu, H.; Han, R. *Arab. J. Chem.* **2017**, 10, S3595-S3602.
28. Thirumalisamy, S.; Subbian, M. *BioResources* **2010**, 5 (1), 419-437.
29. Koçer, O.; Acemioğlu, B. *Desalin. Water Treat.* **2015**, 1-17.
30. Lagergren, S. *Kung. Sven. Vetén. Hand.* **1898**, 24, 1-39.
31. Ho, Y. S.; McKay, G. *Chem. Eng. J.* **1998**, 70 (2), 115-124.
32. Weber, W.J.; Morris, J.C. *J. Sanit Eng. Div.* **1963**, 89, 31-59.
33. Jiang, X.; Sun, Y.; Liu, L.; Wang, S.; Tian, X. *Chem. Eng. J.* **2014**, 235, 151-157.
34. Mihăilescu, M.; Negrea, A.; Ciopec, M.; Davidescu, C. M.; Negrea, P.; Narcis Duțeanu, N.; Rusu, G. *Sci. Rep-UK* **2019**, 9:8757.
35. Bhadusha, N.; Ananthabaskaran, T. *E-J. Chem.* **2011**, 8 (4), 1696-1707.

 ORCID

 <https://orcid.org/0000-0002-0728-2747> (B. Acemioğlu)